DESIGN CONSIDERATIONS WHEN APPLYING LARGE COMPRESSOR SYNCHRONOUS MOTORS TO AN SVC CONTROLLED WEAK POWER SUPPLY SYSTEM

Paper No. PCIC-92-41

Lance G. Grainger, P. Eng., Sr. Member
Grainger Electrical Research Ltd.
8603 - 16 Avenue
Edmonton, Alberta, T6K 2A4

Jack P. Leuw, P. Eng., Member
Trans Canada Pipeline Ltd.
435 Silver Grove Drive
Calgary, Alberta, T3B 4T2

Abstract - **Three 7000 HP synchronous motors driving 360 RPM hydrogen compressors were applied to a refinery with a utility supply consisting initially of one 138 kV feeder with large source impedance. The utility plans to add a second feeder at 230 kV within two years. The system voltage is stabilized with two 40 MVAR Static Var Compensators located at the refinery. Utilizing standard compressor designs, the 6 Hz motor current pulsations were large enough to exceed utility flicker limits. In addition there was a process requirement that the motors ride through an upstream fault which could be cleared in 7 cycles. To meet these conditions a large flywheel had to be added to the compressors to smooth the pulsations. This exacerbated starting times. An added complication was that the pulsation frequency of the motors coincided with the response time of the static var compensator controls, leading to a potential for positive feedback destabilizing the compensator. To analyze the problems required developing a transient electrical model of the motor, and a dynamic torque pulsation model of the motor-compressor-flywheel system. The results from the models were then combined to establish the watts and vars at the pulsation peaks and valleys. This then permitted the use of readily available commercial loadflow programs to calculate the magnitude of the voltage variations on the supply system.**

I. INTRODUCTION

When a large motor is used to drive a reciprocating compressor, applying it to a weak power system involves additional engineering design work. This may be compounded by reactive compensation equipment used by the supply authority to increase the voltage stability of their supply system. The applications engineer must be concerned not only with the capacity and response of the supply system, but also, as described in [1] and [2], with the complications introduced by the pulsating nature of the load. The motor application design problems fall into the following categories:

1. Limiting the flicker caused by the compressor pulsations;
2. limiting the flicker caused by motor starting;
3. protecting the motor from shaft torque transients due to utility reclosures;
4. ensuring the motor and compressor can "ride through" supply disturbances so as not to interrupt the user's process;
5. ensuring the motor pulsating current does not de-stabilize the power system's static var compensators; and
6. setting the motor pole slipping protection to avoid spurious trips during "ride through" swings.

To achieve successful results requires close co-operation among the compressor manufacturer, motor manufacturer, electric utility, client project engineer and the consulting companies. A number of design teams are involved, each of which has it own area of responsibility. Actual motor data such as the "V-curves" will not be available, hence initial design studies must use typical and assumed parameters. These can be refined as more detailed data becomes available over the life of the project.

The project which led to this paper is a refinery designed to process heavy crude oil by cracking it with hydrogen. This process required three 7000 HP hydrogen compressors to be installed, which collectively formed half the refinery's electrical load. The plant was sited in an area remote from the utility's generation which resulted in high source impedances making the plant susceptible to voltage flicker. The design called for two 240 kV transmission lines to supply a 240 kV ring bus at the plant's main station. Two 50 MVA transformers stepped the voltage down to 25 kV for in-plant distribution, and 4.16 kV was selected by the owner as the required voltage for medium voltage motors. To stabilize voltage during faults, the utility and the owner decided to install two 40 MVAR static var compensators , one on each 25 kV bus. The motor captive transformers were located in the Hydrogen Unit, close coupled to the motor 5 kV starting breakers. The 25 kV feeders from the main station to the transformers were 1200 feet long, and the 5 kV feeders from the starter to the motors were 700 feet long Figure 1 gives the plant configuration .

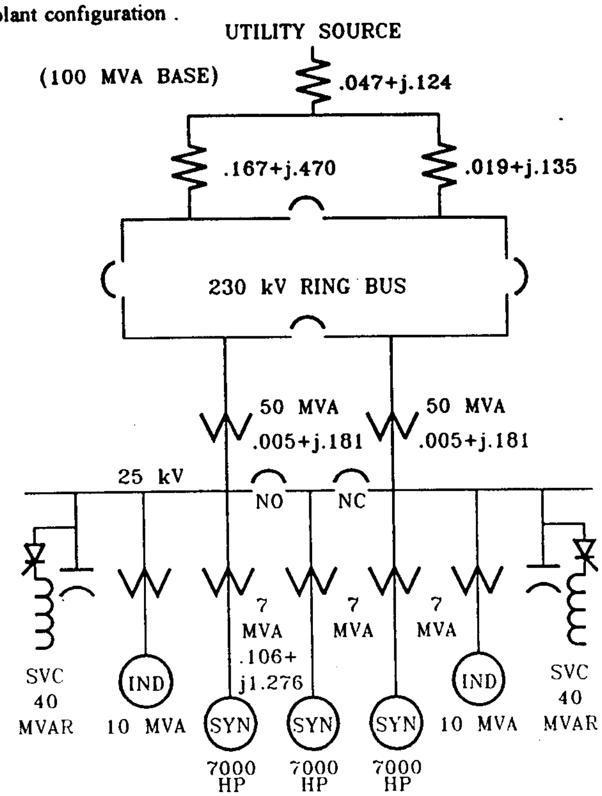

Fig. 1 - Plant Power Supply & Distribution

There are many permutations and combinations of items that can be manipulated to control the voltage drop at the motor and the voltage drop at the plant main bus. The presence of the SVC at the main bus meant there would be good control for voltage in general, but there was a time window lasting 4 cycles during which the SVC would be

92-CH3186-4/1/92/0000-0131 $03.00 ® 1992IEEE

delayed in reacting to relatively small voltage dips due to motor starting or compressor pulsation. This delay did not apply to severe voltage dips due to upstream faults as one of the SVC's primary missions was to provide fault stability. There was a concern that short duration dips would cause the plant high pressure sodium lighting to turn off, particularly in cold weather (less than -20 C). Initially it was suggested the SVC be sent a "pre-act" signal to provide 20 MVAR during a motor start, but subsequent design work showed this option to be unnecessary. The captive transformer impedance, cable feeder type, and motor inrush current were adjusted to minimize voltage drop at the motor. This impacted the purchase specifications and equipment costs as normal manufacturers' design ranges for impedances could not be used. The final required impedance for the transformers was 7% - 7 1/2%, which was higher than usual, and the motor inrush was limited to 350%, which was lower than usual.

The final design utilized the SVC to hold the main 25 kV bus at rated voltage, and permitted the motor voltage to dip to only 85 % of rated. This voltage was chosen by calculation of the available starting torque needed to accelerate the compressor-motor-flywheel combination within 13 seconds, a start time number worked out in consultation with the motor manufacturer. A computer load flow run was used to determine the motor voltage during starting.

Limiting flicker for reciprocating compressor pulsations has been solved for decades by using a flywheel, and is well known to compressor vendors. To limit current pulsation to the NEMA MG-1 guideline of 66% required only 85,000 lb-ft^2 total train inertia, and most, if not all, of this could be supplied by the motor rotor. This plant had a much higher than usual supply impedance. The result was the 6 Hz pulsation flicker on the main bus exceeded the utility's contractual flicker limits. The amount of flicker was doubled when two compressor's ran in unison (ie. within +/- 4 poles of 20 poles). Several schemes were looked at to slip the second motor's rotor until dephasing was achieved. An inexpensive field weakening scheme would have been possible with a slip ring, separately excited motor, but this was not an option as the motor was required to operate in the Division 2 area outside a Hydrogen Plant. As a flywheel was required for other reasons, this proved to be the cost effective answer to the pulsation flicker problem.

The requirements imposed to provide "ride through" process stability in the event of a fault on the 240 kV transmission lines required a larger fly wheel which required heavier bearings, a larger shaft, more iron in the motor, and a higher starting torque. Initial stability studies performed by an outside consultant indicated 350,000 lb-ft^2 would be required to provide this "ride through". The impact on the motor - flywheel - compressor cost was significant and not anticipated by the motor vendors who assumed the NEMA MG-1 criteria during preliminary budget enquiries. To obtain the additional inertia required adding a heavy flywheel which sagged the rotor shaft, requiring it to be beefed up, and the bearings had to support more weight. This was exacerbated by the long shaft motor design which provided a stator which could be moved back to provide in situ access to the rotor. The larger flywheel also increased starting times for the units. More detailed calculations resulted in the inertia being lowered to 251,000 lb-ft^2, resulting in considerable cost saving.

During the design it was identified that greater stability could be achieved with an exciter which could rapidly boost excitation. It was also requested by the designers of the static var compensator (SVC) that a "constant var" exciter be used to minimize interactions with the SVC. In the end a constant current exciter was selected as it was the least expensive, yet maintained a high pull out torque at light loads. The "constant var" exciter would have weakened the motor field considerably at light loads, affecting stability. The ideal exciter would have incorporated a high ceiling voltage and controls to increase excitation as motor terminal voltage fell, but this unit was more expensive and was found to not be required.

II. PULSATION FLICKER

Torque pulsations in the load create current pulsations in the motor which interact with the supply impedance to create voltage flicker. An example of this is shown in figure 2 which is for a 360 RPM motor. Note that one revolution of the compressor impacts 10 electrical cycles of current.

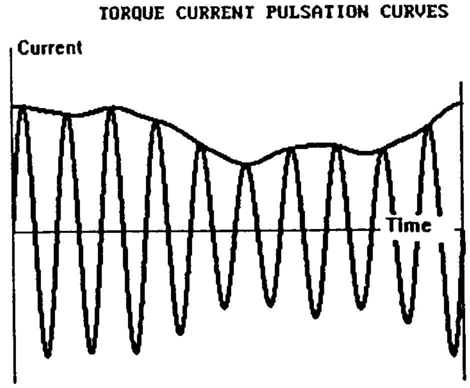

Figure 2 - Effect of Load Pulsation on Motor Current

To relate flicker frequency to RPM in 60 Hz systems, use the formula:

$$f_{FLICKER} = \frac{MOTOR\ RPM}{60}\ Hz \qquad (1)$$

Utilities limit the amount of flicker they will accept by referring to charts similar to fig. 2. These apply both to motor starting and compressor related pulsations.

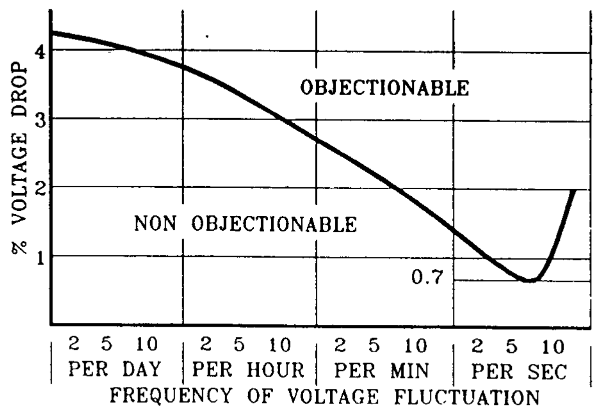

Fig. 3 - Typical Utility Flicker Limits

Hydrogen compressors run at 300 to 360 RPM, placing them in the 5 to 6 Hz. zone, where only 0.7% flicker is allowed. Using traditional "X-factor" methods (referred to in NEMA MG-1 as "C-factor") for determining flicker do not allow for the capacitive effects of leading motor current on system voltages.

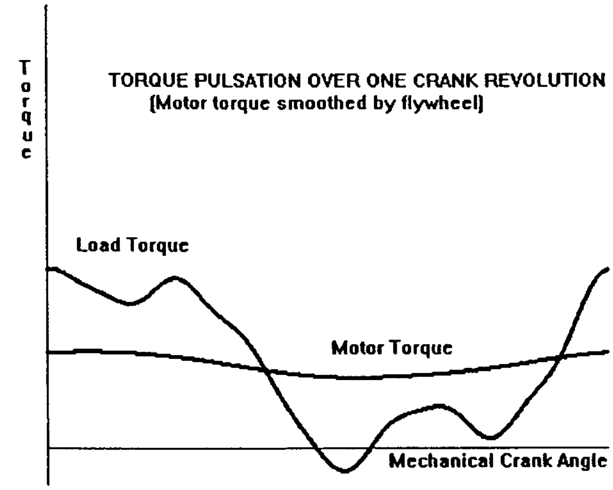

Fig. 4 - Torque Pulsation Versus Crank Angle

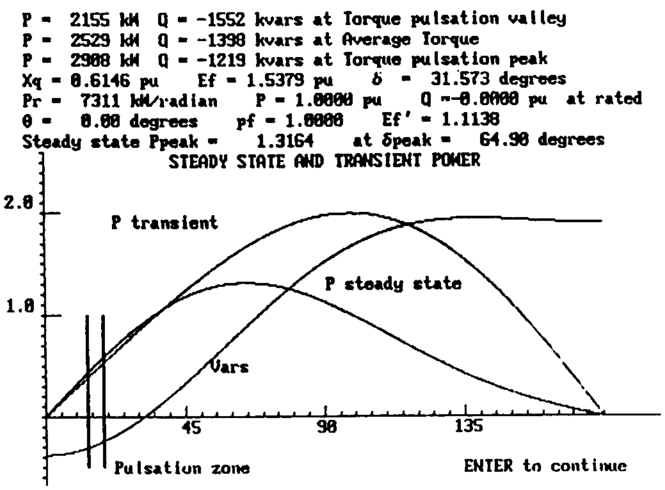

Fig. 5 - Motor Power Curves

III. STARTING FLICKER

Starting of large motors is well described in [3] and [4] with respect to the starting voltage dips imposed on the system, and the oscillatory torques occurring during starting. The added complication for motors with large flywheels is the additional starting time they require. To calculate starting time the starting torque curves were divided into a number of linearized segments. Within each segment

$$T_{ACCEL} = \frac{T_{MOTOR(K)} + T_{MOTOR(K+1)} - T_{LOAD(K)} - T_{LOAD(K+1)}}{2} \quad (15)$$

The motor torques (but not the load torques) must be corrected for actual starting condition voltage at the motor terminals by

$$T_{ACTUAL} = T_{RATED}\left[\frac{V_{ACTUAL}}{V_{RATED}}\right]^2 \quad (16)$$

Motor torque curves and compressor no-load torque curves are available from the vendors. What is not documented, however, is the added torque required by a compressor started in "by-pass" mode. In this mode the discharge is valved to the suction to permit the free flow of gas during starting. This by-pass loading is a function of the square of the compressor speed, and for hydrogen and natural gas machines will reach as high as 35% of the compressor's full load rating at rated RPM. With these corrections applied, starting time can be calculated from:

$$\sum \Delta t = \frac{gf}{2\pi} wk^2 \sum \frac{\Delta N}{T_{ACCEL}} \quad (17)$$

provided suitable intervals are selected for ΔN . The preliminary studies indicated the motor would see a 15 % voltage dip during starting and that the acceleration time would be 12 seconds. This data was given to the motor manufacturer so they could adjust their design damage curve, if necessary, to accommodate the conditions. The final motor damage curve permitted 13 second operation of the motor at locked rotor while operating with 85% voltage. This provided a good margin between the normal starting trace and the damage curve to set the protective relay trip.

IV. RECLOSURE PROTECTION

Should the motor breaker remain closed during the power utility's reclosing of a line after a fault has been cleared, it is possible for a motor to be subjected to high shaft transients. In this event, the best way to detect separation from the supply is to monitor motor frequency with an under frequency relay. The reclosure times are available from the utility protective relay engineers and may vary from a few cycles if the plant is close to major generation, to a few seconds. Rearranging (17), and using an average value for load torque, the speed reduction during the reclosure delay can be calculated. The underfrequency relay can be set to trip at about half the anticipated reduction.

$$\Delta N = \frac{T_{AVG}}{\Delta t (wk^2)}\left[\frac{2\pi}{gf}\right] \quad (18)$$

V. RIDE THROUGH STABILITY

To understand the motor behaviour for ride through stability, refer to Fig 6 (a) (b) and (c) showing the d-q diagrams for the pre-fault, faulted, and post-fault motor conditions.

Note that the direct axis current is leading the terminal voltage in steady state, changes during the fault to lag the voltage behind the transient reactance by 90 degrees, then during the post fault rotor swings changes again, but now lags the terminal voltage when the swing is at its maximum. This latter condition requires careful assessment when setting the motor power factor relay. The machine is in "motoring mode" before and after the fault, but is in "generating mode" during the fault. This means (40) must be used before and after the fault, and (50) during the fault.

Another complication is introduced by the pulsating nature of the compressor load. With reference to Fig. 4 it can be appreciated that the severity of the swing depends upon the angle of the compressor crank at the time the fault occurs. As the rotor of the motor is constantly in motion with respect to the stator the initial values of rotor angle δ_0 and rotor velocity ω_0 change and this affects stability.

$$X = \frac{(0.746)(wk^2)(RPM^4)}{(f)(P_r)(10^8)} \tag{2}$$

To arrive at more accurate answers requires a detailed analysis of the machine combined with load flow studies. First the manufacturer's torque data is converted to a Fourier series. Refer to table 1 for data, and note that the worst case pulsation was at half load .

$$T_{AVG} = \frac{1}{m}(T_1 + T_2 + T_3 + \ldots + T_m) \tag{3}$$

$$a_n = \frac{2}{m}(T_1 \sin n\,\theta_1 + \ldots + T_m \sin n\,\theta_n) \tag{4}$$

$$b_n = \frac{2}{m}(T_1 \cos n\,\theta_1 + \ldots + T_m \cos n\,\theta_n) \tag{5}$$

m = total number of points on the torque curve
n = harmonic order

$$Q_n = \sqrt{a_n^2 + b_n^2}\text{, harmonic magnitude} \tag{6}$$

$$\psi_n = \tan^{-1}\left(\frac{b_n}{a_n}\right)\text{, harmonic angle} \tag{7}$$

$$T_m = T_{AVG} + \sum_{n=1}^{8} Q_n \sin(n\,\omega_c\,t + \psi_n) \tag{8}$$

$$\omega_C = 2\,\pi\,f_{FLICKER} \tag{9}$$

The electric torque seen by the motor after smoothing by the flywheel can be calculated from:

$$T_e = T_s\,\delta_c + \sum_{n=1}^{8} T_{dn}\left(\frac{d\delta_c}{dt}\right)_n \tag{10}$$

Refer to the appendices for the derivation of damping torque T_d and the mechanical rotor to stator angle δ_c. Synchronizing torque T_s can be obtained from the manufacturer. If given as synchronizing power, P_r, then

$$T_s = \left[\frac{P_R}{\omega_C}\,\frac{Newton\ metres}{radian}\right]\left[.7325\,\frac{foot-lbs}{Newton\ metres}\right] \tag{11}$$

Generally the procedure is to calculate T_e at every mechanical degree of crank angle to determine the "maximum torque" and the "minimum torque", and the corresponding angles at which they occur. These angles are then converted from mechanical degrees to electrical degrees by:

$$\delta = \delta_C\,[Pole\ Pairs] \tag{12}$$

Once the angles associated with the maximum and minimum torques are determined, they can be used to calculate the power and reactive volt-amps required by the motor for those angles.

To accomplish this requires solving the motor power equations at the two angles of interest to obtain the corresponding watts and vars.

$$Q = -\frac{V_t E_F}{x_d}\cos\delta + \frac{V_t^2}{x_d}\cos^2\delta + \frac{V_t^2}{x_q}\sin^2\delta \tag{13}$$

$$P = \frac{(V_t \sin\delta)\,V_t\cos\delta}{x_q} - \frac{(V_t\cos\delta - E_f)\,V_t\sin\delta}{x_d} \tag{14}$$

This data can then be used in an ordinary load flow program to determine the changes in system voltage on busses of interest. Typically, the direct axis quantities X_d ,X'_d, and T'_{do}, and the synchronizing power P_r are available early in the design process, while the quadrature axis quantities X_q, E_f, and E'_f are not available. These latter parameters can be solved iteratively from the equations in Appendix I.

A worst case source impedance was assumed of 187 MVA (one line out). Torque versus crank angle preliminary data is shown in Table 1. The following preliminary motor data was used:

1. P_r = 7312 kW / radian
2. P = 5100 kW
3. X_d = 1.31
4. X'_d = 0.5
5. Starting / Pull In / Pull Out Torques = 50 / 40 / 150 %

Table 1 - Compressor Torque Data

ANGLE θ DEG	TORQUE FULL LOAD LB-FT	TORQUE HALF LOAD LB-FT	ANGLE θ DEG	TORQUE FULL LOAD LB-FT	TORQUE HALF LOAD LB-FT
10	130606	97453	190	38447	-13723
20	118241	91452	200	32629	-8855
30	109622	87941	210	42438	5767
40	110870	85353	220	61282	11808
50	110109	81558	230	67983	16586
60	111192	81718	240	77382	22055
70	119766	86662	250	83191	25131
80	133904	96604	260	88753	18301
90	140844	93200	270	72931	11830
100	124639	81321	280	58549	7619
110	113555	73146	290	53592	8400
120	110152	69459	300	60809	15450
130	103767	58558	310	71007	26957
140	96710	42489	320	78051	39196
150	89486	28718	330	88387	53745
160	83130	16532	340	102116	70103
170	78474	2861	350	119787	88364
180	57055	-7677	360	130606	102697

The flywheel size was increased until the load flow results indicated a flicker of less than 0.7% on the 230 kV ring bus with both compressors running in unison. The final system inertia was selected at 251 000 lb-ft^2, giving a flicker of 0.64% . The results calculated by the two programs for pulsation and motor power are shown in Figures 4 and 5.

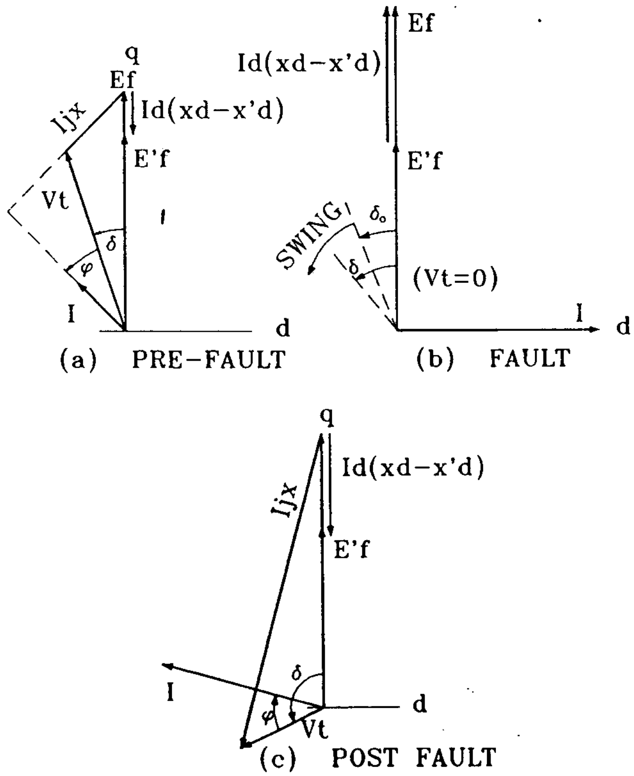

Figure 6 - Motor d-q Diagrams
(a) Pre-Fault (b) Faulted (c) Maximum Post-Fault Swing

The angle and velocity were calculated at 30 degree crank intervals and used to determine the worst case for ride through stability. It was determined the machine would ride through a fault which occurred upstream of the 230 kV ring bus and which was cleared within 7 cycles by the ring bus breakers.

Table 2 - Effects of Torque Pulsation On Motor Stability
(Full Load With 252,000 lb-ft^2 Inertia)

CRANK POSITION DEGREES	δ_0 ELECTRICAL DEGREES	ω_0 ELECTRICAL RAD/SEC	FAULT RIDETHRU CYCLES
30	38.423	+ 6.845	7.5
60	38.337	-19.456	7.6
90	37.800	-61.617	7.9
120	36.718	-87.184	8.2
150	35.505	-83.046	8.2
180	35.527	-52.698	7.9
210	34.227	+ 9.804	7.6
240	34.585	+35.091	7.3
270	35.133	+45.208	7.3
300	35.997	+80.265	7.0
330	37.168	+81.773	7.0
360	38.097	+45.019	7.3

VI. STATIC VAR INTERACTION

The static var compensator (SVC) was applied to the system for two reasons:

1. To provide voltage stability to the supply system during a fault.
2. To provide assistance during the starting of the large plant motors.

The starting studies indicated the plant 25 kv voltage would dip 0% with the assistance of the 40 MVAR SVC, and would dip 8% with no SVC assistance and one supply line out. The dip was 4% with both lines operational. It was also determined that the SVC had a 4 cycle delay (based upon 60 Hz) in reacting to a substantial voltage dip hence the system would undergo a transient starting dip for this brief duration. Various schemes were discussed to pre-act the SVC on a motor start, but due to the physical separation of the Hydrogen unit from the SVC location, and the added complexity to the SVC firing controls, this was not implemented in the design. The net result was that the utility flicker limits shown in Figure 3 could not be met during an outage of one of the two 230 kV supply lines to the plant, and this became a matter that was resolved between the owner and the utility in their power contract.

Another concern was the SVC reaction to the steady state 6 Hz. voltage flicker of 0.7 % created on the 25 kV system by the compressors. The SVC was initially planned to be set with a full range compensation (-40 MVAR) in response to a 5% negative voltage variation, or 32 MVAR/kV. The SVC had no capability to provide positive (inductive) MVARS. The 4 cycle delay in a 60 Hz system becomes a 0.4 cycle delay in a system oscillating at 6 Hz. This effectively created a 144 degree phase shift in the voltage correction provided by the SVC. Figure 7 shows the interaction of the SVC and motor with the power system. In effect the supply impedance between the source and the 25 kV bus acts as the open loop transfer function, the gain of the SVC acts as the feedback loop transfer function (with limits on its range), and the perturbations in complex power caused by the compressor pulsations act as the disturbance.

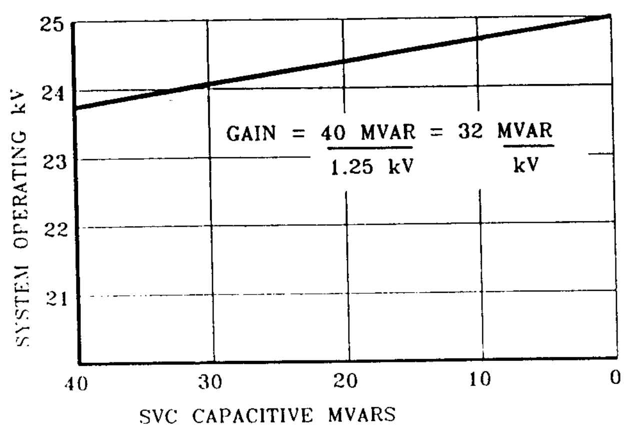

Figure 7 - SVC Operating Range

Design studies showed the system voltage pulsation was made worse by the interaction with the SVC. With the SVC off line, the pulsation on the 25 kV bus was 179 volts. As shown in figure 8 this increased to 600 volts with the SVC on line, abrogating the flicker limits set by the utility. With the gain set at 32 MVAR / kV the SVC operated between 0 and -4 MVAR at a 6 Hz frequency. Note in the figure how the SVC "kicks in" when 80 % of the negative lobe of the disturbing signal has transpired. This delay caused capacitors to be applied at an inappropriate time, boosting the voltage instead of bucking it. This concern was brought to the attention of the SVC manufacturer. One possible solution was to introduce a "dead band" into the SVC control circuitry such that it would ignore small perturbations in voltage.

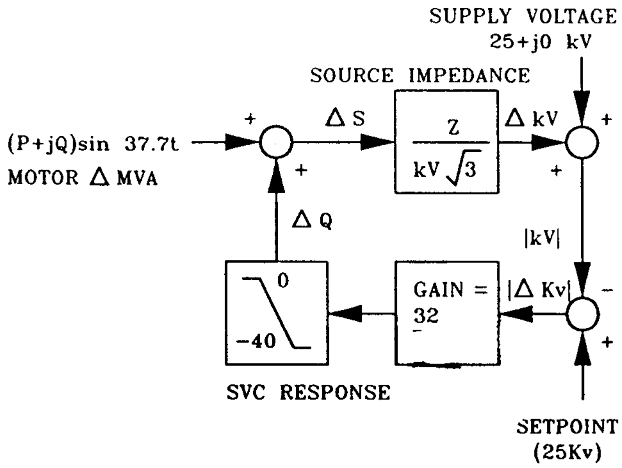

Figure 8 - SVC Interaction With The Motor

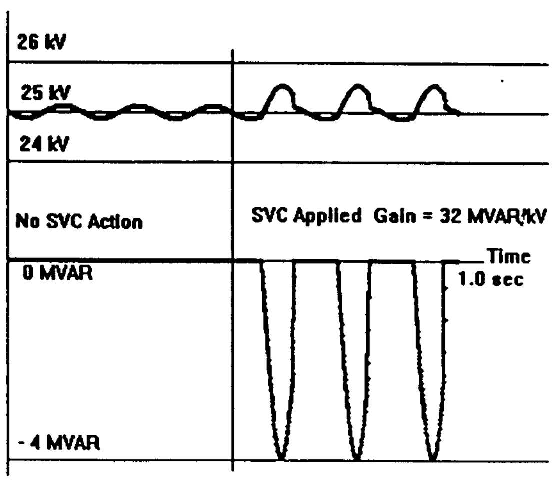

Figure 9 - Variation in Bus Voltage and SVC MVARS

VII. SLIP PROTECTION

Protection against motor pole slipping is normally provided by a power factor relay (ANSI Device 55). This relay has both time delay (typical 0.2 to 1.0 seconds) and power factor set points (typically 0.6 to 1.0 lagging). The time delay setting must be longer than the anticipated fault clearing time, and preferably should include enough post fault time to allow the first swing to recover. If the relay is to be used as backup for loss of excitation protection, the power factor should be set not greater than 0.8 to pickup when the motor is behaving like an induction motor. These two constraints, may not match the behaviour as illustrated in Fig. 6 (c). Part of the swing study should identify the angle by which current lags voltage during the post fault swing, and the time duration of the condition. This information is required by the protection engineer so he can match the relay requirements to the motor behaviour. If the relay is not set properly it may cause a trip during a fault "ride through" condition bringing all the expence of providing a flywheel to naught.

VIII. CONCLUSION

The pulsating nature of reciprocating compressor loads adds complication to system analysis. More detailed system models are required to increase confidence in relay settings, comply with utility flicker limits, provide process ability to "ride through" upstream faults, and to prevent destabilizing interactions from occurring between voltage stabilizers and the process driver motors.

This paper has identified some of the methods required to prepare such models and has shown how to apply them to solve the discussed problems. The result of good engineering is a good process plant.

APPENDIX I - STEADY STATE MOTOR EQUATIONS

Neglecting resistance in the motor:

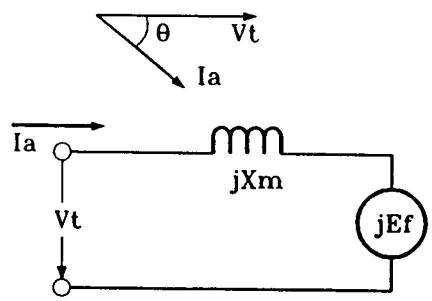

Figure 10 - Steady State Equivalent Circuit

$$V_d = -V_t \sin\delta \tag{19}$$

$$V_q = V_t \cos\delta \tag{20}$$

$$I_d = -I_a \sin(\theta + \delta) \tag{21}$$

$$I_q = I_a \cos(\theta + \delta) \tag{22}$$

Summing the voltage drops around the equivalent circuit

$$V_t = I_a jx_m + E_f \tag{23}$$

Expressing the machine reactance voltage in d-q components

$$I_a jx_m = jI_q x_q + jI_d x_d \tag{24}$$

Placing all components on the d-q diagram and using the d-axis as the reference, expressions can be written by inspection

$$V_d + jV_q = -I_q x_q + jI_d x_d + jE_f \tag{25}$$

Equating the direct-axis components

$$V_d = -I_q x_q \tag{26}$$

$$I_q = \frac{-V_d}{x_q} = \frac{V_t}{x_q} \sin \delta \quad (27)$$

$$x_q = \frac{V_t}{I_q} \sin \delta \quad (28)$$

Equating the quadrature-axis components

$$V_q = I_d x_d + E_f \quad (29)$$

$$I_d = \frac{V_q - E_f}{x_d} = \frac{V_t \cos \delta - E_f}{x_d} \quad (30)$$

$$E_f = V_t \cos \delta - I_d x_d \quad (31)$$

Complex Power

$$S = V_t I_a^* = (V_d + jV_q)(I_d - jI_q) \quad (32)$$

Watts $$P = I_q V_t \cos \delta - I_d V_t \sin \delta \quad (33)$$

Vars $$Q = I_d V_t \cos \delta + I_q V_t \sin \delta \quad (34)$$

Solving in terms of reactance and voltages

$$P = \frac{E_f V_t}{x_d} \sin \delta + \frac{V_t^2}{2} \left(\frac{x_d - x_q}{x_d x_q} \right) \sin 2\delta \quad (35)$$

By definition synchronizing power per radian

$$P_R = \frac{dP}{d\delta} = \frac{E_f V_t}{x_d} \cos \delta + V_t^2 \left(\frac{x_d - x_q}{x_d x_q} \right) \cos 2\delta \quad (36)$$

The corresponding torques can be derived from

$$P = T\omega_M \quad (37)$$

Reluctance Torque $$T_{reluctance} = \frac{V_t^{\ 2}}{2\omega_M} \left(\frac{x_d - x_q}{x_d x_q} \right) \sin 2\delta \quad (38)$$

Excitation Torque $$T_{excitation} = \frac{E_f V_t}{x_d \, \omega_M} \sin \delta \quad (39)$$

APPENDIX II - TRANSIENT STATE MOTOR EQUATIONS

The motor is very resistant to being pulled out of synchronism by short duration load disturbances. A useful model for a motor in the transient state is to define some internal voltage E'_f which changes very little during a short duration disturbance.

$$E_f' = E_f - I_d (x_d - x_d') \quad (40)$$

In a salient machine with amortisseur windings

$$x_q' \approx x_q \quad (41)$$

Transient power is derived in a manner similar to steady state power.

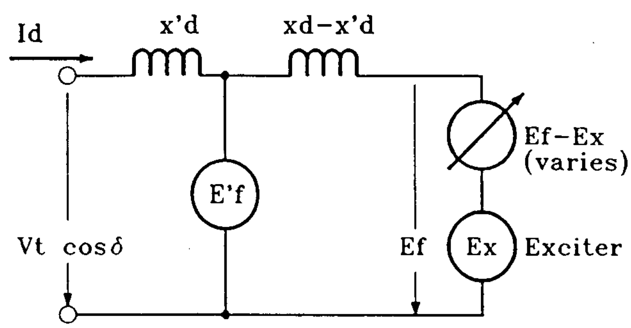

Figure 11 - Transient Equivalent Circuit

$$P' = \frac{E_f' V_t}{x_d} \sin \delta - \frac{V_t^2}{2} \left(\frac{x_q - x_d'}{x_q x_d'} \right) \sin 2\delta \quad (42)$$

The short circuit time constant $$\tau_d' = \frac{x_d'}{x_d} \tau_{do}' \quad (43)$$

d-axis resistance can be calculated from $$R_d = \frac{x_d'}{2\pi f \tau_d'} \quad (44)$$

Modifying the short circuit time constant for external impedance

$$\tau_z' = \frac{x_d' + x_e}{2\pi f (R_d + R_e)} \quad (45)$$

Prior to a transient disturbance the per unit exciter voltage equals the steady state per unit value of the field voltage.

$$E_x = E_{fss} \quad (46)$$

During a fault the voltage behind the transient reactance changes in accordance with the short circuit time constant.

$$\Delta E_f' = \frac{E_x - E_f}{\tau_z'} \Delta t \quad (47)$$

After the fault is cleared the voltage behind the transient reactance changes in accordance with the open circuit time constant.

$$\Delta E_f' = \frac{E_x - E_f}{\tau_{do}'} \Delta t \quad (48)$$

The current varies from about one per unit into the motor prior to a fault, to about four per unit leaving the motor during a fault. The rate of change of current is dictated by external circuit inductance, external voltage and the voltage behind the transient reactance.

$$\Delta I_d = \frac{V_e - E_f'}{\left(\frac{x_d' + x_e}{2\pi f} \right)} \Delta t \quad (49)$$

During a fault, the field voltage swings to maintain constant flux linkages and (40) must be rewritten for generator action.

$$E_f = E_f' + I_d (x_d - x_d') \quad (50)$$

For a constant current exciter, the exciter voltage remains steady, but for a voltage regulating exciter, the exciter voltage will boost in accordance with the exciter's time constant and rated ceiling voltage.

$$E_x = E_{fss} + (E_c - E_{fss})\left(1 - e^{-\frac{t}{\tau_x}}\right) \tag{51}$$

APPENDIX III - DYNAMIC ANALYSIS MOTOR EQUATIONS

The dynamic motor-compressor system can now be modeled as a flywheel with various torques acting upon it. The rotational inertia of the system absorbs and gives up kinetic energy thus the electric torque, T_e, is smoothed as compared to mechanical torque, T_m. Note that these equations use the mechanical value of angle denoted by the subscript c (for compressor).

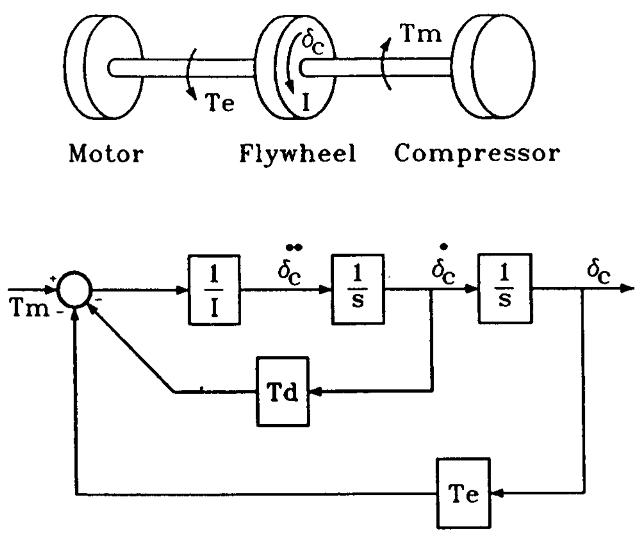

Figure 12 - Motor and Compressor Dynamic Model

Rotational inertia
$$I = \frac{wk^2}{g} \tag{52}$$

$$I\frac{d^2\delta_c}{dt} + T_e = T_m \tag{53}$$

Breaking T_e into its damping torque T_d and synchronizing torque T_s components gives:

$$I\frac{d^2\delta_c}{dt^2} + T_d\frac{d\delta_c}{dt} + T_s\delta_c = T_m \tag{54}$$

divide by T_s
$$\frac{I}{T_s}\frac{d^2\delta_c}{dt^2} + \frac{T_d}{T_s}\frac{d\delta_c}{dt} + \frac{T_s}{T_s}\delta_c = \frac{T_m}{T_s} \tag{55}$$

$$\delta_c = \frac{T_m}{(T_s - I\omega_c^2) + jT_d\omega_c} \tag{56}$$

Converting to polar form

Magnitude
$$|\delta_c| = \frac{T_m}{\sqrt{(T_s - I\omega_c^2)^2 + (T_d\omega_c)^2}} \tag{57}$$

Angle
$$\phi = \tan^{-1}\left(\frac{T_d\omega_c}{T_s - I\omega_c^2}\right) \tag{58}$$

Equation (57) and (58) show the general form of the equations, but are not directly applicable as they do not account for the harmonic components of T_m and T_d. The damping torque term

$$T_d\frac{d\delta_c}{dt} = \sum_{n=1}^{4} T_{dn}\left(\frac{d\delta_c}{dt}\right)_n \tag{59}$$

At each of the first four harmonics, the damping torque constants T_{dn} and their associated harmonic angle ϵ_n are:

Harmonic magnitude
$$T_{dn} = \frac{\lambda_n T_s}{\omega_c} \tag{60}$$

Halberg in [1] provides data for typical damping factors λ_n

Harmonic angle
$$\epsilon_n = \tan^{-1}(n\lambda_n) \tag{61}$$

Which modifies (58) to

$$\phi_n = \tan^{-1}\left(\frac{n\omega_c T_{dn}}{T_s - n^2\omega_c^2 I}\right) \tag{62}$$

Substituting (8) (60) (61) and (62) into (57) the mechanical angle can therefore be calculated at any point by means of the harmonic summation:

$$\delta_c = \frac{T_{avg}}{T_s} + \sum_{n=1}^{8}\left(\frac{Q_n\sin(n\omega_c t + \psi_n - \phi_n)}{\sqrt{(T_s - n^2\omega_c^2 I)^2 + (n\omega_c T_{dn})^2}}\right) \tag{63}$$

$$\frac{d\delta_c}{dt} = \sum_{n=1}^{8}\left(\frac{n\omega_c Q_n\cos(n\omega_c t + \psi_n - \phi_n)}{\sqrt{(T_s - n^2\omega_c^2 I)^2 + (n\omega_c T_{dn})^2}}\right) \tag{64}$$

The electric torque seen by the motor after smoothing by the flywheel is:

$$T_e = T_s\delta_c + \sum_{n=1}^{8} T_{dn}\left(\frac{d\delta_c}{dt}\right)_n \tag{65}$$

APPENDIX IV - MOTOR SWING EQUATIONS

The mechanical power required by the motor load is obtained from (8).

$$P_m = \omega_c T_m \tag{66}$$

The electrical power during a fault is

$$P' = 0 \tag{67}$$

The electrical power during a transient is described by (40), provided proper conversions are made from per unit to three phase quantities. The difference between mechanical and electrical power causes the motor rotor to swing. The electrical angular acceleration, angular velocity, and angle can be solve recursively. For any step "k" in the iteration:

$$\Delta P_{(k)} = P_{(k)}' - P_{m(k)} \tag{68}$$

$$\alpha_{(k)} = \frac{180 f(\Delta P_{(k)})}{H(KVA_{RATED})} \tag{69}$$

$$H = \frac{kW - \sec}{kVA} = 0.231 \frac{(wk^2)(RPM^2)(10^{-6})}{kVA} \tag{70}$$

$$\omega_{(k+1)} = \omega_{(k)} + \alpha_{(k)} t \tag{71}$$

$$\delta_{(k+1)} = \delta_{(k)} + \omega_{(k)} t - \frac{1}{2} \alpha_{(k)} t^2 \tag{72}$$

The initial value for the angle can be found from (63) and using (12) to convert from mechanical to electrical degrees. The initial value for angular velocity can be found by solving (63) for small time periods immediately preceding and following the time of interest.

$$\omega_{(t)} \approx \frac{\Delta \delta}{\Delta t} = \frac{\delta_{(t+\Delta t)} - \delta_{(t-\Delta t)}}{2 \Delta t} \tag{73}$$

TABLE OF REFERENCES

[1] M. N. Halberg, "Calculating The Size of Flywheel Required for a Synchronous Motor Driven Reciprocating Compressor", in *Conf Rec 1956 Sept. 10-12 ASME Meeting in Denver*, ASME Paper 56-F-18

[2] P. G Cummings, "Power and Current Pulsations of an Induction Motor Connected to a Reciprocating Compressor", *IEEE Trans. Ind. App.*, vol. IA-14, No. 3, pp. 213-219, May/June 1978

[3] G. L. Godwin and E. F. Merril, "Oscillatory Torques During Synchronous Motor Starting", *IEEE Trans. on Ind. & Gen. App.*, vol IGA-6, No. 3, pp. 258-265, May/June 1970

[4] G. S. Sangha, "Capacitor-Reactor Start of Large Synchronous Motor on a Limited Capacity Network", *IEEE Trans. Ind. App.*, Vol IA-20, No. 5, pp. 1337-1343, Sept./Oct. 1984

[5] E. W. Kimbark, *Power System Stability - Vol. III - Synchronous Machines*, John Wiley & Sons Inc., New York, 1956